JOURNAL OF MATERIALS SCIENCE 24 (1989) 4168–4175

Toughness properties of a three-dimensional carbon–epoxy composite

VALÉRIE A. GUÉNON, TSU-WEI CHOU, JOHN W. GILLESPIE Jr
Department of Mechanical Engineering, Center for Composite Materials, University of Delaware, Newark, Delaware 19716, USA

The three-dimensional (3D) orthogonal interlocked fabric contains through-the-thickness reinforcement in order to enhance the interlaminar fracture toughness of the composite. The interlaminar fracture toughness of a carbon–epoxy orthogonal interlocked fabric composite was experimentally determined by use of the recently developed tabbed double cantilever beam specimen. The data reduction methods applicable to these tests and materials and the interpretation of the results were discussed. The results of critical strain energy release rate, G_{Ic}, were compared to those of a two-dimensional (2D) laminate having the same in-plane structure. The energy-dissipating crack propagation processes were described. The in-plane fracture toughness of the 3D fabric was experimentally measured and compared to that of the 2D laminate. The through-the-thickness fibres were found to create a ten-fold increase in interlaminar toughness, and a 25% improvement in the in-plane fracture toughness.

1. Introduction

Traditional laminated composite structures exhibit low interlaminar fracture toughness and are susceptible to delamination when subjected to interlaminar stress concentrations. Interlaminar stresses may arise from manufacturing defects, impact damage or geometric discontinuities such as free edges, notches, ply terminations, bolted and bonded joints [1]. Delamination growth is particularly sensitive to compressive loadings [2, 3]. Local stiffness and strength reductions might initiate catastrophic failure of the structure. Improvements in damage tolerance to date have focused on utilizing tougher matrices [4] or interleafing concepts [5]. Through-the-thickness reinforcement provides an alternative approach to substantially increasing the damage tolerance of composite structures [6–13].

Textile fibre geometries having through-the-thickness reinforcement are called three-dimensional (3D) fabrics. Several types of 3D fabrics have been developed and provide unique properties characteristic of the microstructure. Among them, the "orthogonal interlocked fabric composite" (see Fig. 1) provides fibre architectures aimed at retaining in-plane performance while enhancing out-of-plane properties, by including a small amount of through-the-thickness reinforcement. One other advantage of 3D fabric composites during manufacturing is that the fabric preform can be handled easily without much change in the distribution of fibres. The through-the-thickness yarns bind the preform and hold the in-plane fibres together.

It is important to quantify the influence of the z-direction reinforcement on the material performances to assess fully the trade-off between in-plane and interlaminar properties in the design of fabric composite structures. The z-direction fibres were found to be detrimental to the in-plane tensile and compressive properties [6, 10–12]. The presence of the z-direction fibres creates matrix pockets that reduce the volume fraction of in-plane fibres relative to the analogous two-dimensional (2D) laminates. A high fibre volume fraction cannot be obtained in the composite processing without deforming the z-direction yarns upon consolidation and potentially suppressing their beneficial effect on the out-of-plane properties. Because of the fibre geometry, the mode I fracture toughness is the most improved. Ogo [6] observed a twelve-fold increase in mode I interlaminar fracture toughness with stitching, but only an 8% increase in mode II.

In this paper, the effects of the 3D fabric geometry on the interlaminar and in-plane fracture behaviour of the orthogonal fabric composite were evaluated. The mode I interlaminar fracture toughness, G_{Ic}, and the in-plane critical stress intensity factor, K_{Ic}, were compared with those of a 2D laminate having a comparable material system and in-plane stacking sequence.

2. Materials systems

The orthogonal interlocked fabric composite is made of T300/3501-6 carbon/epoxy by Fiber Materials Inc. FMI. The fabrication of the preform is a one-run process, where the lay up of in-plane fibres and the introduction of the z-direction fibres are done simultaneously. This is different from stitching, where the in-plane fibres are first laid-up and then stitched together. The interlocking process avoids the cutting of fibres, as it occurs in the stitching process. However, it creates matrix pockets – visible in Fig. 1 – which lower the fibre volume fraction.

0022–2461/89 $03.00 + .12

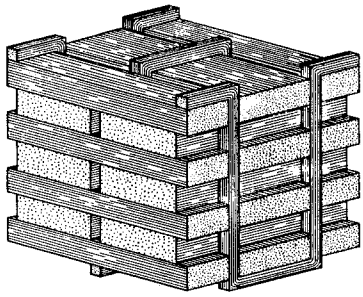

Figure 1 The orthogonal interlocked fibre.

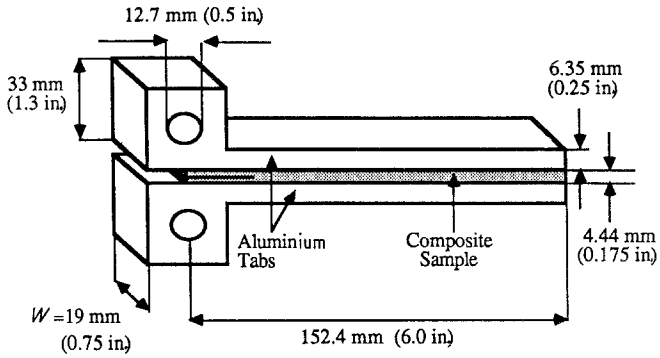

Figure 3 The tabbed DCB specimen.

Fig. 1 shows the ideal fibre configuration of the orthogonal interlocked fabric composite. The material can be described as a [0°/90°] laminate in which some through-the-thickness yarns are interlaced. The in-plane tows are 6 K and the through-the-thickness tows are 1 K (i.e. 6000 and 1000 fibres per tow, respectively). The spacing between two z-direction yarns in both plate directions is 2.8 mm and the plate contains about 13 z-direction yarns per cm^2. The total number of plies is 27, with 14 plies in the x-direction and 13 in the y-direction. However, the weaving process causes the y-direction plies to be slightly thicker than the x-direction plies. Therefore, approximately the same amount of fibres run in both in-plane directions. The preform was received from the fabricator in the form of preimpregnated 190 mm × 343 mm plates where the resin was in a semi-cured stage. The plates were cured in an autoclave with a vacuum bag procedure, at 350° C and 586 kPa, following the recommended cure cycle for Hercules 3501-6 resin system. The overall fibre volume fraction is 50%, while the volume fraction of fibres running in the z-direction – defined in [12] – is 1%.

3. Interlaminar fracture toughness

3.1. Testing procedure

The double cantilever beam (DCB) test is a test method for pure mode I interlaminar fracture toughness that has been successfully applied to unidirectional composite laminates [14–17]. The DCB test specimen is shown in Fig. 2. However, this test method was found not to be applicable to the 3D fabric composite [12]: one of the specimen's arms failed commonly in bending and the crack deviated in the presence of the z-direction yarns instead of propagating in a self-similar manner between the plies, as observed in the DCB testing of unidirectional laminates. Therefore, a new DCB specimen configuration was developed for testing the mode I interlaminar fracture toughness of the 3D composite [12]. This specimen, termed "tabbed DCB", uses long aluminium tabs bonded along each side of the specimen, as shown in Fig. 3.

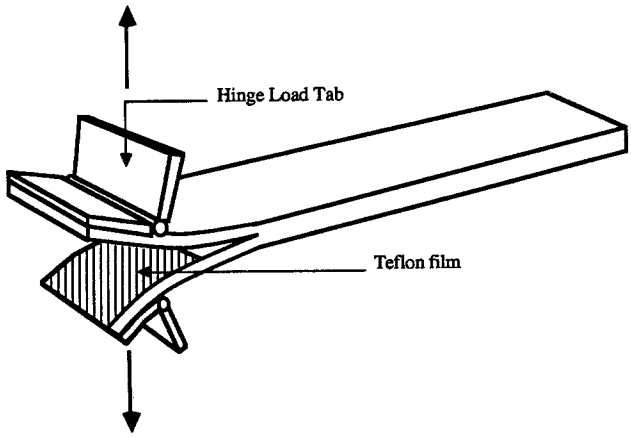

Figure 2 The regular double cantilever beam test specimen.

The tabbed DCB specimen was pin-loaded in tension in a screw-driven Instron static testing machine in displacement-controlled mode. The specimen was loaded until the crack extended about 6 mm. Then, the machine was stopped to record the actual crack length and the specimen was unloaded until a zero load reading was observed. The procedure was repeated several times. The crack length was defined as the distance between the load application point and the crack tip, and measured with a caliper (0.0254 mm precision) after the specimen was taken out of the machine grips. About ten loading/unloading sequences were performed on each specimen. The tests were initated at low cross-head speed (0.254 mm min^{-1}) to induce slow delamination growth. The cross-head speed was increased up to 1.27 mm min^{-1} with increasing crack length. Each cross-head speed change was done before starting a new loading cycle. The load point displacement was measured by means of the actual stroke of the machine grips.

On two of sixteen specimens, the crack growth mechanisms were observed by means of a travelling optical microscope along the specimen's side. The observed face was covered with a thin layer of white spray paint and the locations of the z-direction tows were marked with a pencil.

3.2. Discussion of the load–deflection curves

An example of the load–deflection curves obtained from testing the orthogonal interlocked fabric composite with the tabbed DCB is shown in Fig. 4. The chart was displaced after each unloading for the purpose of easier reading.

The first two loading sequences are perfectly linear, while the subsequent loading curves show a dramatic change in slope at low load level (10 to 20% of the critical load). After this initial kink, the curve is linear until the crack starts propagating. In order to evaluate a possible effect of the specimen fixture upon the load–deflection behaviour, a dummy specimen, made of two aluminium tabs bonded together without the composite sample, was tested. The load–deflection

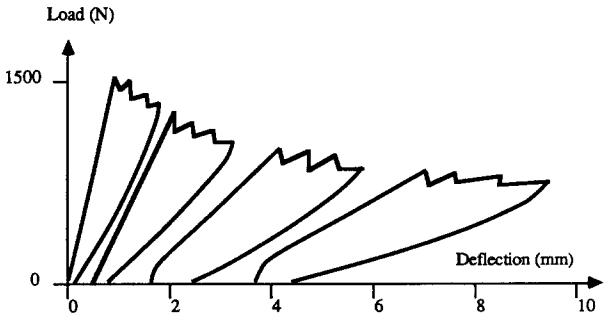

Figure 4 Example of a load–deflection curve.

curve obtained from this test showed the same initial kink as in Fig. 4. Therefore, the initial non-linearity was not due to the composite sample itself. The reasons for this kink are not clear. However, the thick bond line at the aluminium/composite interface might be responsible for it. In order to obtain a good adhesive strength between the aluminium tabs and the composite sample, deep scratches were made into the aluminium tabs surfaces. This procedure was necessary to avoid failure of the bonded interface, but it significantly increased the amount of adhesive at the interface. The loading of the epoxy bond line, therefore, appeared to be responsible for the initial kink on the load–deflection curves.

The curves showed a non-linear unloading sequence and an appreciable permanent deformation after unloading. The permanent deformation was also observed with the optical microscope: the crack tip did not completely close after unloading. These features were explained by the crack closure process of the 3D fabric composite. As shown in Fig. 5, the fracture surface shows the z-direction yarns protruding out of the plane of fracture. Most of the z-direction yarns did not break in the plane of the crack. Instead, they fractured near the outer surface of the specimen where they are curved by the weaving process, and then debonded and pulled-out. During unloading, the pulled-out yarns do not resume their initial locations and therefore progressively undergo compressive stresses that lead to a non-linear unloading behaviour and a permanent deflection of the specimen after a zero load is reached.

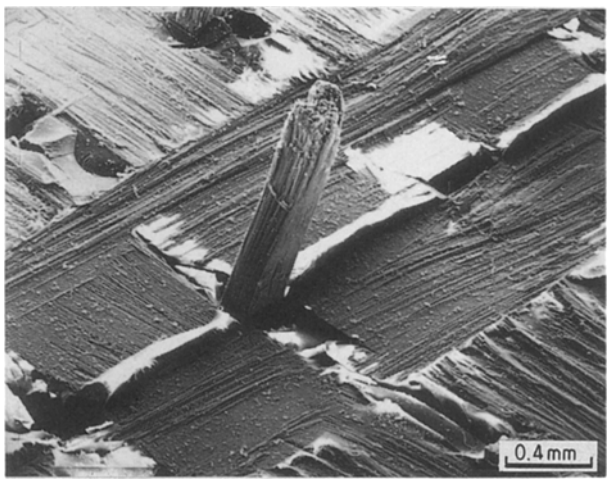

Figure 5 Fracture surface of the orthogonal interlocked fabric composite showing pulled-out yarns.

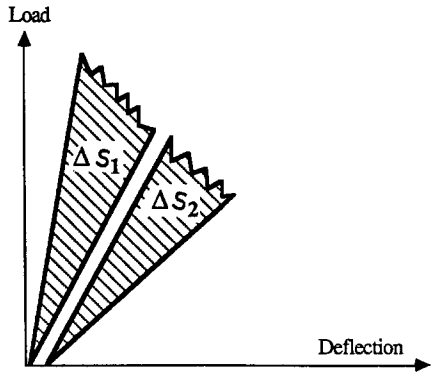

Figure 6 Area measurements in the regular DCB test.

On a few specimens, certain loading/unloading sequences exhibited some non-linearity due to the yielding of the aluminium tabs because the applied stresses exceeded the yield stress of the aluminium. Because the plastic deformation of the aluminium absorbs a large amount of energy, the measured G_{Ic} would have been overestimated. Therefore, these data were discarded. Geometric non-linearities were not responsible for the observed non-linearity, because the beams were very stiff and the critical displacements were a small percentage of the specimen thickness. The friction of the grips did not affect the load–deflection curves: oil-lubricated pins led to the same load–deflection curves as non-lubricated ones.

The crack propagation part of the curves exhibited a "stick-slip" behaviour, consisting of successive load drops followed by crack arrest. Unstable crack propagation was also occasionally observed, as indicated by some sudden load drops.

3.3. Data reduction

3.3.1. Area method

The most appropriate data reduction method for the 3D fabric composite is the area method, that is based on energy considerations. By definition, the interlaminar fracture toughness, in terms of mode I critical strain energy release rate, G_{Ic}, is equal to the energy required to extend a pre-existing crack

$$G_{Ic} = \Delta U/\Delta A \quad (1)$$

where U is the total strain energy stored in the test specimen and A is the area of crack extension. In a regular DCB test of a unidirectional laminate, the energy ΔU required to extend the crack surface from A to $A + \Delta A$ is the area between the loading and unloading curves, ΔS, as shown in Fig. 6. Thus, G_{Ic} is given by

$$G_{Ic}^{i} = \frac{\Delta S_i}{W \Delta a_i} \quad (2)$$

where W is the specimen width, Δa is the crack length increment and i refers to the loading/unloading sequence number.

In order to apply the area method to the orthogonal interlocked fabric composite, a modification to the measured area needs to be made. The crack closure process increases the area inside the loading/unloading curve without contributing to the crack growth energy. This contribution was suppressed, as shown in Fig. 7.

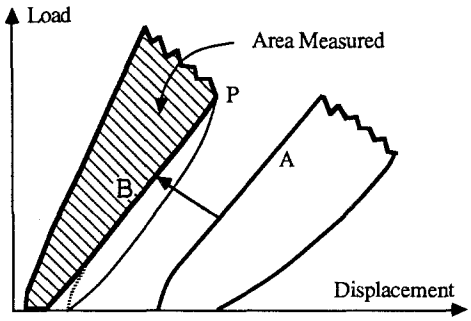

Figure 7 Area measurements in the tabbed DCB test.

The unloading curve of each cycle was approximated by use of the loading part of the subsequent loading cycle. Curve A, on Fig. 7, was superimposed on the previous curve by making it coincide with point P, at which unloading started. The unloading curve was assumed to be linear and thus the initial kink of the loading curve was not reported. The area under curve B was discarded from the area measurement.

3.3.2. Compliance method

The compliance method is based upon linear elastic beam theory. It assumes that each cracked half behaves as a cantilever beam of length a, corresponding to the crack length measured from the loading point. The deflection, δ, of a cantilever beam, according to the strength of materials [18] is

$$\delta = \frac{PL^3}{3E_fI} + \frac{6PL}{5GhW} \quad (3)$$

where P is the applied load, L is the beam length, E_f is the flexural modulus, E_fI is the flexural rigidity of the beam, W is the beam width, h is the beam height and G is the interlaminar modulus. The two terms on the right-hand side of Equation 3 are the bending and shear deflections, respectively. From Equation 3, the compliance, i.e. the ratio of deflection over load, of the double cantilever beam is

$$C = \frac{8a^3}{E_fWh^3} + \frac{12a}{5GhW} \quad (4)$$

It was found [19] that some deflection also occurs because of some rotation at the assumed clamped end of the beam. This contribution to the compliance can be treated as an increase in crack length [19] or as a modification of the bending modulus. Equation 4 can be written as

$$C = Aa^3 + Ba \quad (5)$$

where the constants A and B include this modification. The mode I critical strain energy release rate, G_{Ic}, is defined by the Griffith's criterion of linear elastic fracture mechanics as [20]

$$G_{Ic} = \frac{P_c^2}{2W}\frac{dC}{da} \quad (6)$$

where P_c is the critical load, i.e. the load at which crack propagation occurs. Therefore, G_{Ic} can be obtained for each crack length as

$$G_{Ic} = \frac{P_c^2}{2W}(3Aa^2 + B) \quad (7)$$

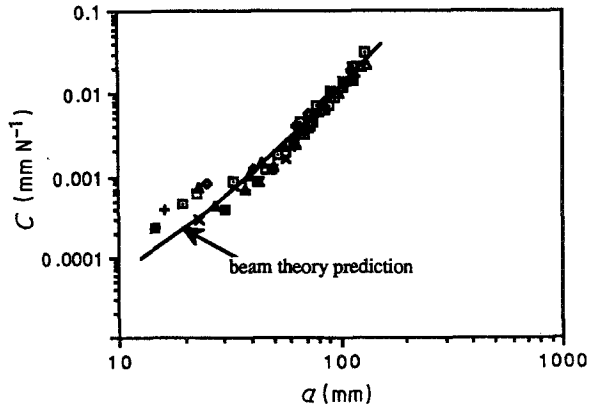

Figure 8 Compliance plotted against crack length.

The compliance–crack length data were obtained from the load–displacement curves of each specimen. Because the initial kink on the curves was not attributed to a composite-related behaviour, it was ignored, and the compliance was measured from the linear part of each loading curve. A least squares fit was applied to the data to determine the values of A and B, which were substituted into Equation 7 for calculating G_{Ic}.

A theoretical prediction of the compliance–crack length curve was done by computing the numerical expression of Equation 4. In order to account for the additional deflection due to the rotation of the beams, a correction to the crack length, a_0, was added in Equation 4. This correction was shown to be equal to 0.6 h [19] with $h = 8.57$ mm. Thus, Equation 4 becomes

$$C = A'(a + 0.6h)^3 + B'(a + 0.6h) \quad (8)$$

where $A' = 2/3E_fI$ and $B' = 12/5GhW$ are similar to the constants A and B, but do not include the modification due to the rotations of the beams. The flexural rigidity of the composite–aluminium beam was calculated as

$$E_fI = E_cI_c + E_aI_a \quad (9)$$

where E_c, E_a, I_c, I_a are the Young's moduli and the moments of inertia of the aluminium and composite parts, respectively, with respect to the neutral axis. $E_c = 56\,812$ MPa [12] and for 6061-T6 aluminium, $E_a = 68.9$ GPa [21]. The interlaminar shear modulus, G, was approximated with the inverse rule of mixtures given in [22]

$$G = h\Big/\left(\frac{h_c}{G_c} + \frac{h_a}{G_a}\right) \quad (10)$$

where G_c, G_a, h_c, h_a are the shear moduli and thicknesses of the aluminium and composite beams, respectively. $G_c = 2.96$ GPa was experimentally determined in [10] and for 6061-T6 aluminium, $G_a = 26.9$ GPa [21]. The numerical expression of Equation 8 was obtained as

$$C = 1.038 \times 10^{-8}(a + 5.16)^3 + 1.70 \times 10^{-6}(a + 5.16) \quad (11)$$

where $A' = 1.038 \times 10^{-8}\,N^{-1}\,mm^{-2}$ and $B' = 1.70 \times 10^{-6}\,N^{-1}$.

Fig. 8 shows some of the compliance–crack length data obtained, together with the theoretical curve

TABLE I Results of interlaminar fracture toughness for the 3D fabric composite

	Method	
	Area	Compliance
Mean G_{Ic} (kJ m^{-2}) (in.lb in^{-2})	3.85 (22.0)	2.66 (15.2)
95 % G_{Ic} (kJ m^{-2}) (in.lb in^{-2})	1.65 (9.43)	1.01 (5.77)
S.D. (kJ m^{-2}) (in.lb in^{-2})	1.12 (6.40)	1.44 (8.23)

from Equation 11. The experimental data agree well with the theoretical curve for crack lengths larger than 40 mm. Below this length, the experimental compliance data are significantly higher than what is theoretically predicted. The reasons for this behaviour are not clear. However, when performing the same test on the aluminium tabs without the composite sample, the compliance data obtained at low crack length were also higher than that predicted from the theory. Some deformation of the bonded interface might be responsible for the higher compliance values at low crack length. The data corresponding to crack lengths below 40 mm were therefore discarded in calculating the average values of G_{Ic} in both the area and compliance methods. In the compliance method, the constants A and B were re-evaluated by applying the least squares fit to the data for crack lengths above 40 mm.

3.4. Results and discussion

Sixteen specimens were tested; 67 data points were obtained from the area method and 88 from the compliance method.

The mean values of G_{Ic} are given in Table I. The critical load data showed a high level of scatter, which resulted in the high scatter in the G_{Ic} results. Because of this scatter, a statistical analysis was applied to the data. A Weibull distribution curve was fitted to the data points, using the software package CEMCAL [23]. The strain energy release rates for a confidence level of 95% are given in Table I.

The experimentally determined A and B constants and the calculated A' and B' constants (see Equation 11) are given in Table II. The A and B constants agree well with A' and B', although the latter do not include the correction due to the rotation of the beams.

The area method gave a significantly higher G_{Ic} than the compliance method. The compliance method only takes into account the energy of crack initiation. In the case of 2D unidirectional laminates, the crack propagation energy is generally equal to the initiation energy, and therefore both methods give similar results. In the 3D fabric composite, the crack propagation energy involves the energetic contribution of several fracture mechanisms [12]: fracture, debonding and

TABLE II Experimentally determined A and B constants and calculated A' and B' constants

A (N^{-1} mm^{-2})	1.063×10^{-8}
B (N^{-1})	1.90×10^{-6}
A' (N^{-1} mm^{-2})	1.038×10^{-8}
B' (N^{-1})	1.70×10^{-6}

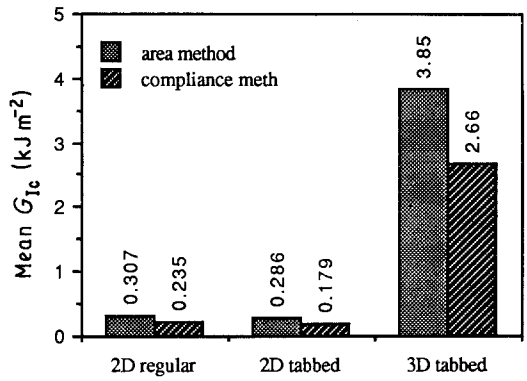

Figure 9 Comparison of the interlaminar fracture toughness of the 3D fabric composite with that of a 2D laminate.

pull-out of the z-direction yarns, bridging of the crack by the z-direction and in-plane fibres, and crack branching. These processes absorb a significant amount of energy which is taken into account by the area method and not by the compliance method. Therefore, the area method gives a higher and more accurate result of G_{Ic} during propagation.

The interlaminar fracture toughness of a two-dimensional (2D) laminate having the same material system, number of plies, stacking sequence, thickness and fibre volume fraction as those of the 3D fabric composite was evaluated. Testing of this material was described previously [12]. The 2D laminate was tested with the regular and tabbed DCB specimens, and both the area and compliance methods were used for data reduction. A reasonable agreement was found between the results of the regular and tabbed DCB tests. For the 3D fabric composite, the area method gave a higher result than the compliance method: because of the 0°/90° stacking sequence, some crack processes such as crack branching and fibre bridging contributed to the crack propagation energy and were taken into account by the area method. Fig. 9 shows the average G_{Ic} results of the 3D fabric compared to those of the 2D laminate. There is more than a ten-fold increase in the mode I interlaminar fracture toughness.

The tabbed DCB specimen is shown being tested in Fig. 10. The observation of crack propagation with the optical microscope gave some understanding of

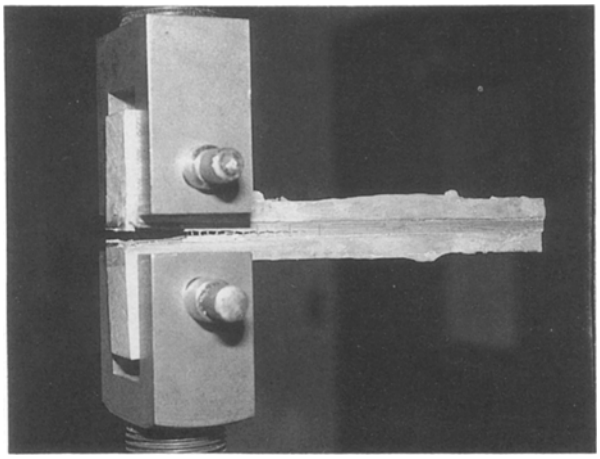

Figure 10 Tabbed DCB specimen being tested.

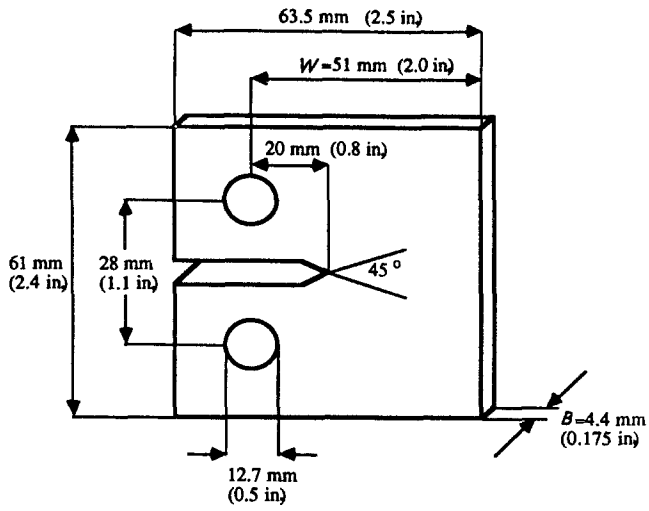

Figure 11 Compact tension specimen configuration.

the dynamic aspect of the crack growth in the 3D fabric composite. As indicated by the jagged crack propagation part of the load–deflection curve (Fig. 4), the crack propagated by small jumps. Stable crack propagation in the matrix was seldom observed. Most of the time, the crack was arrested close to a z-direction yarn after each jump. Therefore, by bridging the crack, the z-direction yarns are responsible for the crack arrests and the "stick–slip" [24] behaviour on the load–deflection curve. Fig. 10 shows the crack profile and the bridging z-direction fibres.

The crack propagated mainly in a self-similar manner. However, the crack frequently branched or deviated from its main direction, sometimes resulting in the simultaneous propagation of two parallel crack fronts over a short length. The crack deviations occurred because of the presence of the z-direction fibres. The crack tended to follow the z-direction yarns' boundaries or was diverted by the presence of pre-existing matrix cracks. These matrix cracks occurred in the resin-rich region surrounding the z-direction yarns due to the release of thermal stresses after curing. As a result of crack branching, in-plane fibre bridging across the crack tip occurred.

Therefore, the z-direction yarns increase the energy required to propagate an interlaminar crack in several ways.

1. Energy is required to fracture, debond and pull-out the z-direction yarns.
2. In the vicinity of a z-direction yarn, crack branching and deviation create additional crack initiation and growth, therefore increasing the absorbed fracture energy.
3. Crack branching and deviation lead to bridging of the crack by in-plane fibres; energy is needed to fracture those bridging fibres.

4. In-plane fracture toughness

The in-plane fracture toughness was experimentally determined in terms of critical stress intensity factor for the orthogonal interlocked fabric composite and was compared to that of the 2D laminate. The testing technique was the same as that used by Friedrich [25]. The compact tension specimen configuration shown in Fig. 11 was adopted.

Two kinds of specimen were tested in order to discern the possible difference between the x- and y-directions of the 3D material. The specimens whose cracks were parallel to the x-direction were called x-specimens, and those with the crack parallel to the y-direction were called y-specimens.

The specimens were loaded in an Instron static testing machine at a cross-head speed of 1.27 mm min^{-1} for the 3D composite [24]. In the 2D laminate, the crack tended to propagate in an unstable manner; therefore, a cross-head speed of 0.254 mm min^{-1} was used. The load-point displacement was measured by means of the actual stroke of the machine grips. The specimen was unloaded until a crack grew approximately 10 mm. The load decreased sharply when this occurred. The new crack length was measured and the cross-head was driven back to the zero load position. The procedure was repeated several times until the crack propagated to about 90% of the specimen's width, W.

The fracture toughness was defined as the value of the stress intensity factor, K_I, at which a crack in the specimen began to grow unstably before being arrested. This occurred at a maximum load, F_c. For the calculation of K_c, the following equation was used [25]

$$K_c = \frac{F_c}{BW^{1/2}} Y(a/W) \tag{12}$$

where B is the specimen thickness, W is the specimen width, a is the crack length and Y is the following geometrical correction factor [25]

$$\begin{aligned} Y(a/W) = {} & 29.6\,(a/W)^{1/2} - 185.5\,(a/W)^{3/2} \\ & + 655.7\,(a/W)^{5/2} - 1017\,(a/W)^{7/2} \\ & + 638.9\,(a/W)^{9/2}. \end{aligned} \tag{13}$$

In the 2D laminate, the crack was very straight, following the longitudinal fibre direction. In the 3D fabric composite, the crack propagated in more of a zig-zag fashion. Also, the crack surfaces of the 3D composite are very rough, as opposed to the smooth crack surfaces of the 2D laminate. The presence of the z-direction fibres and of the matrix pockets cause the crack to deviate from its intended fracture plane and propagate in an irregular manner. The crack always propagated stably in the 3D fabric composite. In the 2D laminate, all speciments had a sudden unstable

TABLE III Results of in-plane fracture toughness test

	Specimen type		
	3D-X	3D-Y	2D
K_{Ic} (MPa m$^{1/2}$)	29.45	28.56	21.22
(p.s.i. in$^{1/2}$)	681.2	660.6	490.8

crack propagation all along their width, W, and therefore gave less data points than the 3D material.

The average critical stress intensity factor, K_{Ic}, was calculated. The data obtained from the machined crack as well as those corresponding to a crack length larger than 85% of the specimen width were discarded in calculating the average K_{Ic}. The summary of results is given in Table III. No significant difference was found between both directions of testing in the 3D fabric composite, because about the same number of fibres lay in each direction as was mentioned earlier. Although a smaller number of data were obtained from the 2D laminate testing, their fracture toughness was 25% lower than in the 3D fabric composite. The z-direction fibres help arrest and deviate the crack, which requires more fracture energy than in the 2D laminate. Therefore, the z-direction fibres have a beneficial effect on the in-plane fracture toughness.

5. Conclusions

1. The interlaminar fracture toughness of the orthogonal interlocked fabric composite was evaluated by using the tabbed DCB specimen. The values of G_{Ic} for the 3D material were compared with those of a 2D laminate. The presence of 1% of through-the-thickness fibres results in a more than ten-fold increase in interlaminar fracture toughness.

2. The load–deflection curves show different features from those of a unidirectional laminate tested with the regular DCB. The initial non-linearity was attributed to the specimen fixture itself; the non-linearity during unloading and the residual deformation after unloading was explained by the crack closure process, which puts the pulled-out z-direction yarns into compression.

3. The area and compliance data reduction methods were used. A modification was made to the area method in order to account for the crack closure process. The compliance data agree well with the beam theory prediction. A high degree of scatter was found in the values of critical load, and therefore in the G_{Ic} results. The compliance method gives much more conservative results than the area method, because all of the observed energy dissipating crack processes were not measured. The area method is therefore more appropriate to determine the interlaminar fracture toughness of the 3D fabric composite.

4. The interlaminar crack propagation processes were observed. The energy dissipating processes related to the presence of the z-direction fibres are: fracture, debonding, and pull-out of the z-direction fibres, crack branching and deviating, and bridging of the crack by a significant amount of in-plane fibres.

5. The in-plane fracture toughness of the orthogonal interlocked fabric composite was evaluated and compared to that of a 2D composite. The z-direction fibres not only increase the interlaminar fracture toughness, but also are beneficial to the in-plane toughness, by arresting and deviating the crack.

Acknowledgements

This work was supported by NASA-Langley Research Center, Hampton, Virginia, through grant number NAG-1-378/ASR. The authors thank Dr Leif A Carlsson and Mr Dale W. Wilson for many helpful discussions, and Mr Touy Thiravong for his help in the experimental work.

References

1. D. J. WILKINS, "The Engineering Significance of Defects in Composite Structures", AGARD Conference Proceeding No. 355 (Elsevier, Essex, 1983).
2. J. W. GILLESPIE Jr, *Comp. Struct.* **2** (1984) 49.
3. R. J. ROTHSCHILDS, J. W. GILLESPIE Jr and L. A. CARLSSON, "Instability Related Delamination Growth in Thermoset and Thermoplastic Composites", ASTM STP 972 (American Society for Testing and Materials, Philadelphia, Pennsylvania, 1988).
4. D. H. HUNSTON, *Comp. Technol. Rev.* **6** (4) (1984) 176.
5. J. E. MASTERS, "Characterization of Impact Development in Graphite Epoxy Laminates", ASTM STP 948 (American Society for Testing and Materials, Philadelphia, Pennsylvania, 1987) pp. 238–58.
6. Y. OGO, Master's thesis, University of Delaware (1987).
7. L. A. MIGNERY, T. M. TAN and C. T. SUN, "The Use of Stitching to Suppress Delamination in Laminated Composites", ASTM STP 876 (American Society for Testing and Materials, Philadelphia, Pennsylvania, 1985) pp. 371–85.
8. A. B. MACANDER, R. M. CRANE and E. T. CAMPONESCHI Jr, "Fabrication and Mechanical Properties of Multidimensionally (X-D) Braided Composite Materials", ASTM STP 873 (American Society for Testing and Materials, Philadelphia, Pennsylvania, 1986) pp. 422–45.
9. H. B. DEXTER and J. G. FUNK, "Impact Resistance and Interlaminar Fracture Toughness of Through-the-Thickness Reinforced Graphite Epoxy", AIAA Paper, 86-1020-CP (1986) pp. 700–709.
10. S. W. FOWSER, Master's thesis, University of Delaware (1986).
11. T. R. GUESS and E. D. REEDY Jr, *Compos. Technol. Res.* 7 (4) (1985) 136.
12. V. A. GUÉNON, T. W. CHOU and J. W. GILLESPIE Jr, Fabricating Composites '87 Conference, SME technical paper, 15–18 September, 1987 Philadelphia, Pennsylvania (SME, Michigan, 1987) EM 87-551; 1–17.
13. L. TASKE and A. P. MAJIDI, in Proceedings of the American Society for Composites, Second Technical Conference, 23–25 September, University of Delaware, Newark, Delaware (Technomic, Lancaster, PA, 1987).
14. J. M. WHITNEY, C. E. BROWNING and W. HOOGSTEDEN, *J. Reinf. Plastics Compos.* October (1982) 297.
15. P. E. KEARY, L. B. ILCEWICZ, C. SHAAR and J. TROSTLE, *J. Compos. Mater.* **19** (2) (1985) 154.
16. D. J. WILKINS, J. R. EISENMANN, R. A. CAMIN, W. S. MARGOLIS and R. A. BENSON, "Characterizing Delamination Crack Growth in Graphite Epoxy", ASTM STP 775 (American Society for Testing and Materials, Philadelphia, Pennsylvania, 1982) pp. 168–83.
17. NASA, "Standard Tests for Toughened Resin Composites", Revised Edition, NASA Reference Publication 1092 ACEE Composites Project Office, Langley Research Center, Hampton, Virginia (1983).
18. E. J. HEARN, "Mechanics of Materials", 2nd Edn, (Pergamon, 1985) International Series on Materials Science and Technology, Vol. 19, p. 271.
19. S. MOSTOVOY, P. B. CROSLEY and E. J. RIPLING, *J. Mater.* **2** (1967) 661.
20. L. A. CARLSSON and R. B. PIPES, "Experimental

Characterization of Advanced Composite Materials" (Prentice Hall, New-Jersey, 1986) pp. 19–21.
21. Reynolds Aluminum Supply Company, Product and Data Catalog (Reynolds, Richmond, Virginia, 1976).
22. S. W. TSAI, Composites Design 1986, Think Composites, p. 11–4.
23. J. M. WHITNEY and J. W. GILLESPIE Jr, "CEMCAL: Composites Experimental Mechanics Calculations", Center for Composite Materials Software, University of Delaware (1987).
24. J. W. GILLESPIE, L. A. CARLSSON and A. J. SMILEY, *Compos. Sci. Technol.* **28** (1987).
25. K. FRIEDRICH, "Microstructure and Fracture of Fiber Reinforced Thermoplastic Polyethylene Terephthalate (Rynite®)" (CCM-80-17 Center for Composite Materials Publication, University of Delaware, 1980).

Received 25 January
and accepted 10 June 1988